CrossMark

Nickel complex engineered interface energetics for efficient photoelectrochemical hydrogen evolution over *p*-Si

Wu Zhou[a,1], Fujun Niu[a,1], Samuel S. Mao[b,c], Shaohua Shen[a,d,*]

[a] International Research Centre for Renewable Energy, State Key Laboratory of Multiphase Flow in Power Engineering, Xi'an Jiaotong University, Shaanxi 710049, China
[b] Institute of New Energy, Science Hall, 1003 Shangbu Road, Shenzhen 518031, China
[c] Department of Mechanical Engineering, University of California at Berkeley, Berkeley, CA 94720, USA
[d] Xi'an Jiaotong University Suzhou Academy, Suzhou 215123, China

ARTICLE INFO

ABSTRACT

Here we report a *p*-Si photocathode decorated with nickel complex Ni(TEOA)$_2$Cl$_2$ (**Ni1**) in acidic aqueous solution (pH = 0.3) for photoelectrochemical (PEC) H$_2$ generation. Compared to bare *p*-Si, *p*-Si/**Ni1** electrode exhibits significantly enhanced PEC performance, with higher cathodic photocurrent and exceptional lower onset potential. A relatively high photocurrent density of 5.57 mA/cm^2 was obtained at 0.0 V vs. reversible hydrogen electrode (RHE) under simulated 1 Sun illumination, which is even comparable to that of *p*-Si/Pt. Furthermore, the highly active *p*-Si/**Ni1** electrode shows a remarkable stability over 24 h. The possible catalysis mechanism of **Ni1** for *p*-Si in the PEC H$_2$ evolution process was also proposed in detail. The excellent PEC performance should be attributed to the **Ni1** engineered *p*-Si/electrolyte interface energetics and the **Ni1** catalyzed water reduction reaction, leading to robust hydrogen generation and excellent PEC stability. The present study made a deep insight into the engineered interface charge transfer and catalyst-driven surface water reduction processes at the semiconductor/electrolyte interface, which could provide some referable guidelines for fabricating highly efficient PEC system for solar H$_2$ generation from the viewpoint of interface energetics engineering with metal complexes.

1. Introduction

Solar hydrogen generation by photoelectrochemical (PEC) water splitting has attracted increasing attentions to get clean and renewable energy [1–3]. The past decades have seen the fast development of versatile photoelectrodes for efficient PEC H$_2$ generation [4–6]. Among these photoelectrodes, Si has attracted intensive attentions due to its earth abundant source, and narrow band gap (E$_g$ = ~1.1 eV), which is relatively well matched to the solar spectrum [7–9]. However, Si tends to form insulated oxide in the presence of water and energetic holes, which will passivate the electrode for PEC applications. Moreover, with the Fermi level pinning at the surface states, which dramatically affects the charge transfer rate in the surface electrochemistry, sluggish reaction kinetics on bare Si surface is also a critical issue for the improvement of PEC performance [10].

For efficient PEC H$_2$ generation, *p*-Si is usually used as photocathode decorated with Pt catalyst [11–13]. Moreover, many efforts have been devoted to improve the stability and efficiency of *p*-Si photocathodes,

including protective layer deposition (e.g., ZnO, Al$_2$O$_3$, SiO$_2$) [14–19] and nanostructure design [20,21]. For example, Li et al. reported a *p*-Si photocathode coated with a thin epitaxial protective layer of strontium titanate (SrTiO$_3$) by molecular beam epitaxy and nanostructured Ti/Pt catalyst, which exhibited a maximum photocurrent density of 35 mA/cm^2 and stability over 35 h in 0.5 M H$_2$SO$_4$ [22]. Boettcher et al. reported *p*-Si microwire arrays coated with a 1.5-nm-thick discontinuous film of evaporated Pt, which displayed a photocurrent density of 7.3 mA/cm^2 at the equilibrium water reduction potential and a fill factor of 0.18 measured under solar illumination [20]. Although these *p*-Si photocathodes exhibited quite good stabilities and efficiencies for PEC H$_2$ generation, the presence of noble metals and the complexity of fabrication processes may hinder their wide application.

Compared with semiconductor materials, metal complexes made of earth abundant elements (e.g., Co, Fe, Ni) are more attractive and promising for catalyzing H$_2$ production due to their high atom utilizations, low cost, and adjustable chemical properties [23]. However, reports on metal complexes modified *p*-Si photocathodes for PEC H$_2$

---

production are still very few. For example, Courtney et al. reported a cobalt dithiolene polymer/p-Si electrode, which exhibited a photocurrent density of 3.8 mA/cm^2 at 0 V vs. the reversible hydrogen electrode (RHE) under simulated 1 Sun illumination [24]. Unfortunately, such current can only sustain for 2 h, indicating the poor durability of cobalt dithiolene polymer/p-Si electrode for PEC H$_2$ production. Moreover, all these reported p-Si/metal complexes photocathodes always required drop-casting or other electrostatic-based deposition techniques to integrate or link molecular catalysts onto p-Si surface. The poor stabilities resulted from the easy delamination of metal complexes from p-Si surface [24] and relatively complicated fabrication methods of p-Si/metal complexes photocathodes would greatly limit their practical applications for PEC H$_2$ generation.

In this study, we decorated the surface of p-Si photocathode by simply and directly adding nickel complex Ni(TEOA)$_2$Cl$_2$ (**Ni1**) into the aqueous electrolyte for efficient PEC H$_2$ production. This **Ni1** decorated p-Si (p-Si/**Ni1**) electrode shows much higher cathodic photocurrent and lower onset potential than bare p-Si in 0.5 M H$_2$SO$_4$ aqueous solution (pH = 0.3) under simulated 1 Sun illumination, which is even comparable to the state of the art p-Si/Pt electrode. Moreover, the p-Si/**Ni1** electrode can keep stable for more than 24 h, without any decrease in photocurrent density. It was indicated that the impressive PEC performance should be attributed to the **Ni1** engineered p-Si/electrolyte interface energetics, leading to the enhanced driving force for electron transfer to p-Si surface and then benefitting the following PEC water reduction, as well as the increased energy barrier for hole transfer to p-Si surface, which prevents the p-Si photocathode from oxidation and then enhances the PEC stability.

2. Experimental

2.1. Preparation of Ni(TEOA)$_2$Cl$_2$

Ni(TEOA)$_2$Cl$_2$ (**Ni1**) was synthesized via a facile solution method according to our previous work [25]. Typically, 0.2 mol of TEOA was dissolved in 100 mL of ethanol and 0.1 mol of NiCl$_2$·6H$_2$O was dissolved in 200 mL of hot ethanol solution respectively. Then they were mixed up and refluxed at 50 °C for 30 min under N$_2$ atmosphere. The resulting suspension was filtered and cooled to room temperature. Finally, the product was collected by centrifugation, which was washed extensively with alcohol and ether and then dried at 45 °C for 8 h in a vacuum oven.

2.2. Preparation of p-Si and p-Si/Pt electrodes

p-Si electrode was prepared according to the literature [20]. Single-crystal p-Si wafers (B-doped, (100) oriented, 0.525 mm thick, 0.5 Ω cm resistivity) were cut into 10 × 10 mm^2 chips and then cleaned ultrasonically with acetone, ethanol and deionized water in order for 15 min, 10 min and 5 min, respectively. Then the chips were dipped into 5% HF for 5 min to remove the natural SiO$_2$. Eutectic gallium-indium alloy was rubbed onto the back side of the chips to achieve Ohmic contact. Conductive silver paint and cooper wire were used to make electrical connections. Electroless deposition was used to deposit Pt on p-Si [20]. Typically, the p-Si chips were immersed in an aqueous solution containing 0.1 mM Na$_2$PtCl$_6$·6H$_2$O and 0.5 M HF for 10 min and then dried under N$_2$ atmosphere at room temperature.

2.3. Photoelectrochemical and electrochemical measurements

LSV (Linear sweep voltammograms), EIS (Electrochemical impedance spectra) and M-S (Mott-Schottky) measurements were conducted on a poten-tiostat (PGSTAT302N, Metrohm Autolab) in a three-electrode cell system. 200 mL of 0.5 M H$_2$SO$_4$ aqueous solution (pH = 0.3) was used as electrolyte and purged with N$_2$ for 10 min before tests. The prepared electrodes were used as working electrodes, a platinum plate was used as counter electrode and an Ag/AgCl electrode

was used as reference electrode, respectively. LSV and EIS were carried out under simulated 1 Sun illumination (a Xe lamp with an AM 1.5G filter, light intensity is 100 mW/cm^2) and M-S measurements were carried out under dark. For **Ni1** decorated p-Si electrodes (p-Si/**Ni1**), **Ni1** complex (0.2 mM) was directly added into 200 mL of electrolyte (0.5 M H$_2$SO$_4$ aqueous solution, pH = 0.3) and stirred for 20 min before (photo)electrochemical tests. As reference, NiCl$_2$·6H$_2$O (0.2 mM) or TEOA (0.2 mM) was directly added into 200 mL of electrolyte (0.5 M H$_2$SO$_4$ aqueous solution, pH = 0.3) and stirred for 20 min before photoelectrochemical tests, to exclude the possibility that the increased PEC activity of p-Si/**Ni1** was due to the Ni^{2+} or TEOA released from **Ni1** complex in 0.5 M H$_2$SO$_4$ aqueous solution.

2.4. Characterization

The obtained **Ni1** complex was characterized by electrospray ionization mass spectrometry (EIS-MS) spectra using AXIMA-CF plus a MALDI-TOF Mass Spectrometer instrument, which exhibits a base peak at 355.1363 corresponding to a intramolecular hydrogen formed structure of [Ni(TEOA)$_2$]$^{2+}$. The single-crystal analysis of **Ni1** complex was performed on a Bruker ApexII CCD diffractometer equipped with graphite-monochromated MoKa (l = 0.71073 Å) radiation. The structure was dealt with direct methods using the SHELXS program of the SHELXTL package and refined by full-matrix least-squares methods with SHELXL, with hydrogen atoms generated geometrically with isotropic temperature factors and anisotropic thermal parameters assigned to all nonhydrogen atoms. The surface chemical components and states of the electrodes were detected by an X-ray photoelectron spectrometer (AXIS Ultra DLD, Shimadzu/Kratos Analytical, Japan) with monochromatic AlKa radiation (150 W, 15 kV, 1486.6 eV) under high vacuum. Fourier transform infrared spectra (FTIR) were recorded on a Bruker Vextex 70 FTIR spectrometer using the KBr pellet technique.

3. Results and discussion

3.1. Photoelectrochemical performance of p-Si/**Ni1**

Ni1 complex was synthesized and characterized according to our previous work [25], see Fig. S1, Table S1 and S2 in Supporting Information. The p-Si electrode was decorated with **Ni1** complex for PEC H$_2$ production, by directly adding **Ni1** complex in 0.5 M H$_2$SO$_4$ solution as electrolyte. Generally, X-ray photoelectron spectroscopy (XPS) and Fourier transform infrared spectroscopy (FTIR) are used to investigate the interaction between metal complexes and p-Si [24,26]. For example, Moore et al. reported the successful grafting of Ni complex on the surface of p-Si, with the presence of intact Ni complex and the vibrational modes of catalyst characterized by XPS and FTIR, respectively [27]. In the present system, interestingly, as shown in Fig. S2, neither XPS nor FTIR spectra of p-Si electrode exhibits any change after **Ni1** decoration by dipping p-Si electrode in 0.5 M H$_2$SO$_4$ solution containing 1 mM **Ni1** for 20 min before characterizations, indicating that **Ni1** can be hardly absorbed or linked onto p-Si. Thus, considering the free motion of **Ni1** molecules in electrolyte and the classic theory for the reaction of molecules [28], it is reasonable to expect that the interaction between **Ni1** and p-Si in the solution might be random collision rather than physicochemical adsorption.

The PEC performance was evaluated by a three-electrode cell system in 0.5 M H$_2$SO$_4$ aqueous solution under simulated 1 Sun illumination. Fig. 1a shows the photocurrent density-potential (J-V) curves of p-Si, p-Si/**Ni1** and p-Si/Pt, respectively. It is obvious that the onset potential (V$_{onset}$, defined as the voltage at which the photocurrent density reaches 1 mA/cm^2) of the p-Si/**Ni1** photoelectrode is +0.11 V vs. RHE, which is more positive than that of the bare p-Si (-0.22 V vs. RHE) and comparable to that of p-Si/Pt (+0.19 V vs. RHE), indicating the excellent hydrogen evolution reaction (HER) activity of **Ni1**. To confirm that the enhanced PEC performance is due to molecular
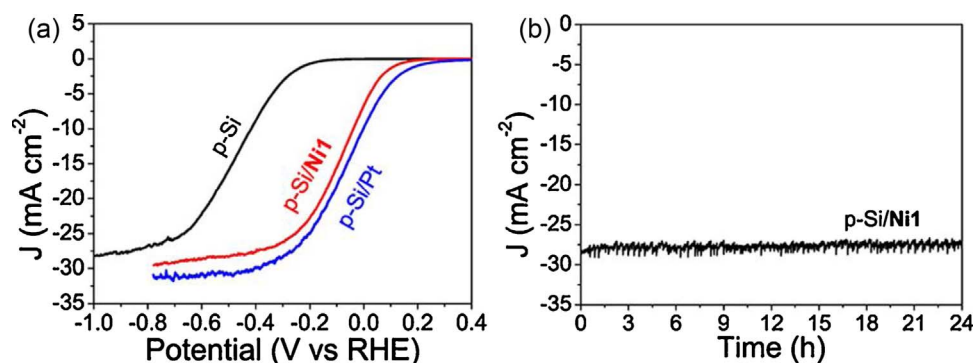
catalyst **Ni1** rather than Ni^{2+} or TEOA released from **Ni1** complex in acidic aqueous electrolyte during the PEC reaction process, a series of control experiments were carried out. As shown in Fig. S3a, there was no obvious shift of V$_{onset}$ or increased saturated photocurrent density for *p*-Si/NiCl$_2$ or *p*-Si/TEOA (NiCl$_2$ or TEOA was added into the electrolyte and stirred for 20 min before PEC reactions) when compared to bare *p*-Si, indicating that neither Ni^{2+} nor TEOA has a positive effect on the enhanced PEC performance of *p*-Si/**Ni1** photocathode. All the results above indicate that **Ni1** is a superior HER cocatalyst and even comparable to the highly efficient Pt. To investigate the stability of the present *p*-Si/**Ni1** photoelectrode, chronoamperometry measurement of *p*-Si/**Ni1** was conducted at a constant potential of −0.4 V vs. RHE (potential which approximately reach the saturated photocurrent) in 0.5 M H$_2$SO$_4$ aqueous solution under simulated 1 Sun illumination. As shown in Fig. 1b, the *p*-Si/**Ni1** photocathode exhibits no decrease in performance metrics after 24 h continuous PEC H$_2$ evolution. The amount of H$_2$ evolved was measured and the Faradic efficiency of the *p*-Si/**Ni1** photocathode for H$_2$ generation was determined. As shown in Table S3 and Fig. S4, the amount of H$_2$ was increased linearly with irradiation time in 24 h PEC reaction. The Faradaic efficiency determined by the ratio of the measured to the calculated amount of H$_2$ evolution was over 96%. Furthermore, XPS analysis was conducted for the *p*-Si/**Ni1** and *p*-Si/NiCl$_2$ electrodes after a chronoamperometry measurement of 24 h. As shown in Fig. S3b, the observed binding energy at 856.0 eV and 873.5 eV suggests the formation of NiO [26,27] on *p*-Si/NiCl$_2$ electrode after long-time PEC reaction. In contrast, there was no peak relative to metal Ni or NiO for *p*-Si/**Ni1** after the chronoamperometry measurement, indicative of the excellent stability of **Ni1** complex in acidic aqueous electrolyte for PEC H$_2$ production over *p*-Si photoelectrode. As shown in Table 1, it is noteworthy that the present *p*-Si/**Ni1** system could stand among the most efficient and stable *p*-Si/metal complexes PEC systems for solar water splitting [24,26,29–31].

The PEC performance of *p*-Si/**Ni1** on the dependence of **Ni1** concentration was investigated by conducting linear sweep voltammetry (LSV) measurements with **Ni1** concentrations varying from 0.01 to 0.16 mM in 0.5 M H$_2$SO$_4$ aqueous solution under simulated 1 Sun illumination (see Fig. 2a). It is obvious that the employment of as little as 0.01 mM of **Ni1** could already dramatically improve the V$_{onset}$ by 235 mV of positive shift, as compared with bare *p*-Si, indicating the

high activity of **Ni1** for HER. With gradually increasing the concentration of **Ni1**, further positive shift of V$_{onset}$ and improved photocurrent density at −0.4 V vs. RHE could be observed (see Fig. 2b), whereas there is no obvious improvement of PEC performance by further increasing the concentration of **Ni1** to be higher than 0.08 mM. These observations indicate that there is a limit of HER rate related to the concentration of **Ni1**, which corresponds well with the limited active sites for *p*-Si in collision theory and the limited surface diffusion rate for HER [28].

3.2. Interface energetics studies

Given the fact that PEC water reduction occurred at the surface of *p*-Si, electrochemical characterizations were employed to investigate the crucial effects of **Ni1** complex on *p*-Si/electrolyte interface for a better understanding of the reason for high PEC performance. Electrochemical impedance spectra (EIS) for bare *p*-Si, *p*-Si/**Ni1** and *p*-Si/Pt photoelectrodes were conducted to investigate the electrodes kinetics in HER as shown in Fig. 3a. The obtained plots were fitted to the equivalent circuit in the inset of Fig. 3a. It is obvious that the R$_{ct}$ of *p*-Si/**Ni1** (256.4 Ω) is much smaller than that of bare *p*-Si (472.7 Ω), indicating that **Ni1** can significantly reduce the charge transfer resistance across the photoelectrode/electrolyte interface. It should be noted that either *p*-Si/**Ni1** or *p*-Si/Pt possesses a similar R$_{ct}$ of ∼250 Ω, which may give some evidenced explanation of the comparable catalytic activity of **Ni1** with Pt for HER.

Mott-Schottky (M-S) analysis was carried out with the bare *p*-Si and *p*-Si/**Ni1** electrodes to further investigate the interface energetics of *p*-Si when **Ni1** was introduced. It has been widely accepted that when a *p*-type semiconductor contacts with aqueous solution, charges in solution will transfer to the semiconductor due to the more positive Fermi level (E$_f$) of solution than semiconductor, leading to the generation of the space charge region with negative charge near the semiconductor surface, which causes the downward bending of band edges. When **Ni1** was introduced to the surface of *p*-Si, as shown in Fig. 3b, the flat band potential (E$_{fb}$) for *p*-Si was positively shifted by 66 mV, indicative of the increased downward band bending of *p*-Si. Thus, the driving force for the electron transfer from the bulk to the surface of *p*-Si was enhanced and then benefiting the following HER (see Fig. 4a), which is in good

Table 1
PEC performance of *p*-Si photocathode decorated with various transition metal complexes.

Metal complexes	J at 0 V vs. RHE (mA/cm^2)	V$_{onset}$ (V)	ΔV$_{onset}$ (mV)	V$_{J = 10}$ (V)	Stability (h)	Reference
[FeFe] complexes	4.8	0.12	–	−0.13	–	[29]
Nickle phosphine	4	0.14	200	−0.2	–	[26]
Cobalt dithiolene	3.8	0.1	430	−0.2	2	[24]
CuMo$_3$S$_4$ clusters	0	−0.07	310	−0.29	0.5	[30]
Mo$_3$S$_4$ clusters	8	0.1	550	−0.07	24	[31]
Ni(TEOA)$_2$Cl$_2$	5.57	0.11	330	−0.03	24	This work

Note: ΔV$_{onset}$ defined as the shift of onset potential compared with bare *p*-Si photocathode. V$_{J = 10}$ defined as the voltage at which the photocurrent density reaches 10 mA/cm^2.
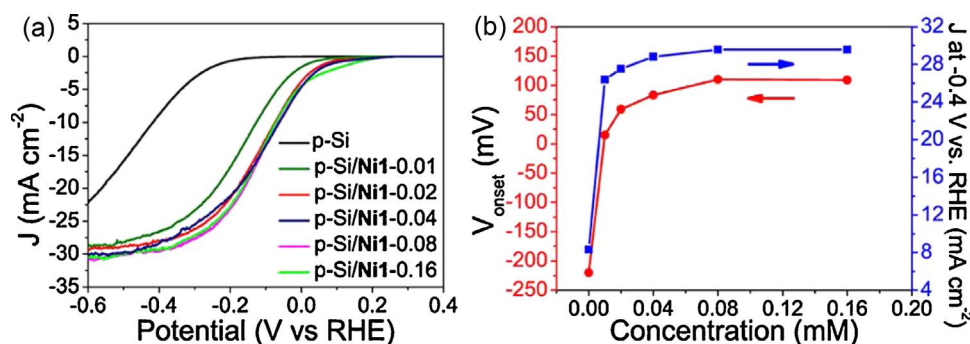
Fig. 2. (a) J-V curves of p-Si/**Ni1** with various concentration of **Ni1** from 0.01 to 0.16 mM. Condition: measured in 0.5 M H_2SO_4 aqueous solution under simulated 1 Sun illumination. Scan rate is 20 mV/s. (b) V_{onset} and photocurrent density at −0.4 V vs. RHE of p-Si/**Ni1** as a function of **Ni1** concentrations.

agreement with the EIS results. Meanwhile, the increased downward band bending would increase the energy barrier to hinder the hole transfer from bulk to surface, preventing p-Si from hole-induced surface self-oxidation, which may account for the good stability of p-Si/**Ni1** even after 24 h PEC reaction. Based on the discussion of EIS and M-S above, it can be concluded that the electron transfer from the bulk to the electrolyte was promoted and the hole transfer from the bulk to the surface was hindered, leading to the enhanced PEC activity and excellent stability.

3.3. Catalysis mechanism of *Ni1* for H_2 evolution

To investigate the catalysis mechanism of **Ni1** for p-Si during the PEC H_2 evolution process, a series of cyclic voltamograms (CV) tests were carried out. As shown in Fig. S4a, **Ni1** shows a semireversible one-electron wave at −0.6 V vs. RHE, which could be assigned to the **Ni1**(II)/**Ni1**(I) redox couple. Considering the positive charges of [Ni(TEOA)$_2$]$^{2+}$ in electrolyte and the more negative CB level (−0.7 V vs. RHE) of p-Si, **Ni1**(II) catalyst tends to get electrons from p-Si and then be reduced to **Ni1**(I), which can be further reduced or protonated in the following HER. However, there is no possible **Ni1**(I)/**Ni1**(0) wave at potential more positive than −1.5 V vs. RHE in the CV of **Ni1**(II), indicating that the two-electron continuous reduction of **Ni1**(II) to **Ni1**(0) is thermodynamically unfavorable. Thus, the resulted **Ni1**(I) species could be protonated to generate **Ni1**(III) molecules. A triggered new catalytic wave at a more negative potential than **Ni1**(II)/**Ni1**(I) couple with the addition of trifluoroacetic acid (TFA) and the negatively shifted potentials of the new wave with the increasing amounts of TFA indicate that **Ni1**(III)-H molecules could be reduced to **Ni1**(II)-H for the following PEC H_2 evolution [32]. Then, to verify whether the **Ni1**(II)-H molecules are protonated or react with other **Ni1**(II)-H molecules to generate H_2, additional CV tests were performed, as shown in Fig. S4b. The photocurrent density performs linear dependence on the concentration of **Ni1**, indicative of the monometallic mechanism [33] in the present p-Si/**Ni1** system, which has been illustrated in other photocatalytic and electrocatalytic H_2 production system [34,35]. Thus, based on the discussion above, the possible catalysis mechanism of **Ni1**

for p-Si in the PEC H_2 evolution process is proposed in Fig. 4b. Typically, under simulated solar illumination, **Ni1**(II) molecules get electrons generated form p-Si and then be reduced to **Ni1**(I), with further protonation and reduction to generate **Ni1**(II)-H molecules, which react with protons in acidic aqueous solution for efficient H_2 evolution by monometallic mechanism.

4. Conclusions

In summary, we demonstrated a novel p-Si/Ni(TEOA)$_2$Cl$_2$ (**Ni1**) photoelectrode by directly adding **Ni1** complex in the acidic solution (pH = 0.3) as electrolyte for high performance PEC H_2 generation. The p-Si/**Ni1** exhibits greatly enhanced PEC activity when compared with bare p-Si, with positively shift of 330 mV in onset potential and increased cathodic current density of 5.57 mA/cm^2 at 0 V vs. RHE, which is even comparable to p-Si/Pt. Furthermore, the present p-Si/**Ni1** photocathode shows remarkable stability for PEC water splitting, without any decrease in current density even after 24 h PEC reaction. The excellent PEC performance should be attributed to the **Ni1** engineered p-Si/electrolyte interface energetics and the increased downward band bending of p-Si, giving rise to promoted driving force for electron transfer from p-Si to electrolyte and then favoring the following PEC H_2 production, as well as increased energy barrier for holes transfer to p-Si electrode surface, which will prevent the hole-induced surface self-oxidation of p-Si. This study successfully fabricated a high performance PEC system for solar H_2 generation and introduced a feasible and facile method to engineer the interface energetics of electrodes and electrolyte using earth abundant metal complex for efficient solar hydrogen production.

Conflict of interests

The authors declare no competing financial interests.
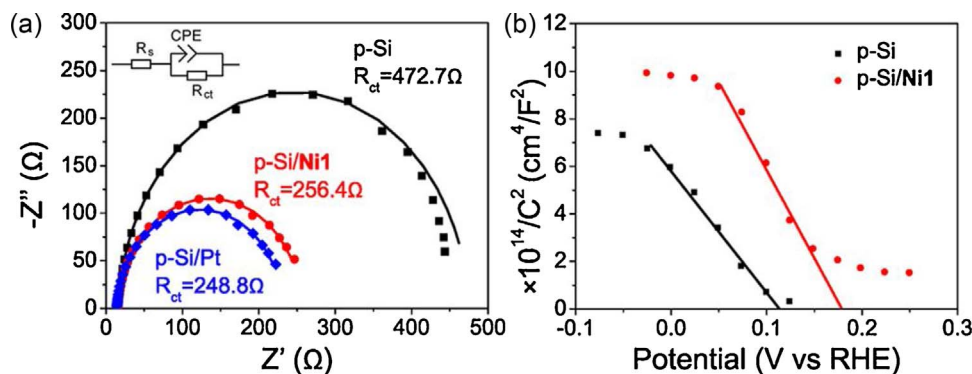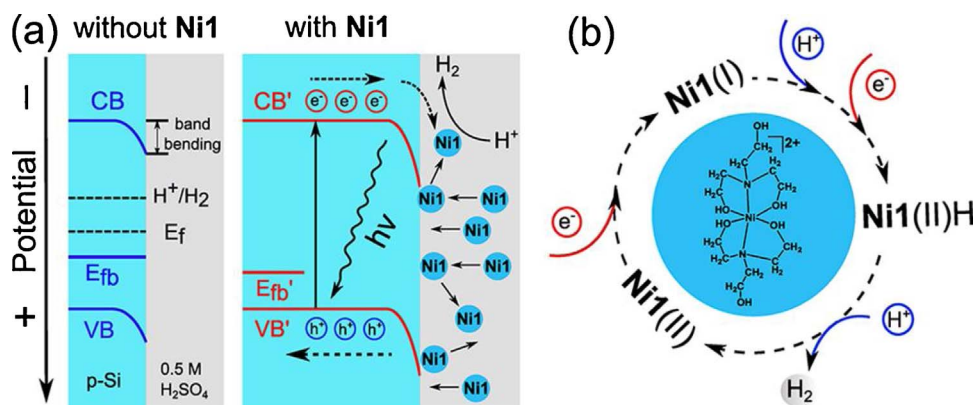
Acknowledgements

Fig. 3. (a) Electrochemical impedance spectra (EIS) and (b) Mott-Schottky (M-S) plots of p-Si, p-Si/**Ni1** and p-Si/Pt. Conditions: EIS were measured at −0.1 V vs. RHE in 0.5 M H_2SO_4 solution under simulated 1 Sun illumination. M-S was measured in 0.5 M H_2SO_4 solution under dark. Scan rate: 20 mV/s.

Fig. 4. (a) The proposed band structure at the *p*-Si/ electrolyte interface without or with **Ni1** in acidic aqueous solution. Blue and red lines represent the conduction band (CB), flat band potential (E_fb) or valence band (VB) of *p*-Si and *p*-Si/**Ni1** respectively in the M-S measurement. (b) The proposed catalysis mechanism of **Ni1** for H₂ evolution. (For interpretation of the references to colour in this figure legend, the reader is referred to the web version of this article.)

Appendix A. Supplementary data

Supplementary data associated with this article can be found, in the online version, at http://dx.doi.org/10.1016/j.apcatb.2017.08.065.

References

[1] D. Hayes, R.G. Hadt, J.D. Emery, A.A. Cordones, A.B.F. Martinson, M.L. Shelby, K.A. Fransted, P.D. Dahlberg, J. Hong, X. Zhang, Q. Kong, R.W. Schoenlein, L.X. Chen, Energy Environ. Sci. 9 (2016) 3754–3769.
[2] Y. Hou, M. Qiu, T. Zhang, J. Ma, S. Liu, X. Zhuang, C. Yuan, X. Feng, Adv. Mater. 29 (2017) 1604480.
[3] W. Li, D. He, S.W. Sheehan, Y. He, J.E. Thorne, X. Yao, G.W. Brudvig, D. Wang, Energy Environ. Sci. 9 (2016) 1794–1802.
[4] J. Li, X. Gao, B. Liu, Q. Feng, X. Li, M. Huang, Z. Liu, J. Zhang, C. Tung, L. Wu, J. Am. Chem. Soc. 138 (2016) 3954–3957.
[5] K.C. Kwon, S. Choi, K. Hong, C.W. Moon, Y. Shim, D.H. Kim, T. Kim, W. Sohn, J. Jeon, C. Lee, K.T. Nam, S. Han, S.Y. Kim, H.W. Jang, Energy Environ. Sci. 9 (2016) 2240–2248.
[6] L.G. Bloor, R. Solarska, K. Bienkowski, P.J. Kulesza, J. Augustynski, M.D. Symes, L. Cronin, J. Am. Chem. Soc. 138 (2016) 6707–6710.
[7] F. Chen, Q. Zhu, Y. Wang, W. Cui, X. Su, Y. Li, ACS Appl Mater. Interfaces 8 (2016) 31025–31031.
[8] W. Cui, S. Wu, F. Chen, Z. Xia, Y. Li, X. Zhang, T. Song, S. Lee, B. Sun, ACS Nano 10 (2016) 9411–9419.
[9] I.H. Kwak, H.S. Im, D.M. Jang, Y.W. Kim, K. Park, Y.R. Lim, E.H. Cha, J. Park, ACS Appl Mater. Interfaces 8 (2016) 5327–5334.
[10] K. Sun, S. Shen, Y. Liang, P.E. Burrows, S.S. Mao, D. Wang, Chem. Rev. 114 (2014) 8662–8719.
[11] W. Wang, H. Wang, Q. Zhu, W. Qin, G. Han, J. Shen, X. Zong, C. Li, Angew. Chem. Int. Ed. 55 (2016) 9229–9233.
[12] J. Kye, M. Shin, B. Lim, J. Jang, I. Oh, S. Hwang, ACS Nano 7 (2013) 6017–6023.
[13] U. Sim, T. Yang, J. Moon, J. Hwang, J. Seo, J. Lee, S. Han, B.H. Hong, K.T. Nam, Energy Environ. Sci. 6 (2013) 3658–3664.
[14] K. Sun, K. Madsen, P. Andersen, W. Bao, Z. Sun, D. Wang, Nanotechnology 23 (2012) 194013.
[15] M.J. Choi, J. Jung, M. Park, J. Song, J. Lee, J.H. Bang, J. Mater. Chem. A 2 (2014) 2928–2933.
[16] D.V. Esposito, I. Levin, T.P. Moffat, A.A. Talin, Nat. Mater. 12 (2013) 562–568.
[17] J.C. Hill, A.T. Landers, J.A. Switzer, Nat. Mater. 14 (2015) 1150–1155.
[18] C. Lee, H.S. Park, J.C. Fontecilla-camps, E. Reisner, Angew. Chem. Int. Ed. 55 (2016) 5971–5974.
[19] N.Y. Labrador, X. Li, Y. Liu, H. Tan, R. Wang, J.T. Koberstein, T.P. Moffat, D.V. Esposito, Nano Lett. 16 (2016) 6452–6459.
[20] S.W. Boettcher, E.L. Warren, M.C. Putnam, E.A. Santori, D. Turner-Evans, M.D. Kelzenberg, M.G. Walter, J.R. Mckone, B.S. Brunschwig, H.A. Atwater, N.S. Lewis, J. Am. Chem. Soc. 133 (2011) 1216–1219.
[21] H. Zhang, Q. Ding, D. He, H. Liu, W. Liu, Z. Li, B. Yang, X. Zhang, L. Lei, S. Jin, Energy Environ. Sci. 9 (2016) 3113–3119.
[22] L. Ji, M.D. McDaniel, S. Wang, A.B. Posadas, X. Li, H. Huang, J.C. Lee, A.A. Demkov, A.J. Bard, J.G. Ekerdt, E.T. Yu, Nat. Nanotechnol. 10 (2015) 84–90.
[23] P. Du, R. Eisenberg, Energy Environ. Sci. 5 (2012) 6012–6021.
[24] C.A. Downes, S.C. Marinescu, J. Am. Chem. Soc. 137 (2015) 13740–13743.
[25] F. Niu, S. Shen, L. Guo, J. Catal. 344 (2016) 141–147.
[26] J. Soe, R.T. Pekarek, M.J. Rose, Chem. Commun. 51 (2015) 13264–13267.
[27] G.F. Moore, I.D. Sharp, J. Phys. Chem. Lett. 4 (2013) 568–572.
[28] M.L. Goldberg, K.M. Watson in Collision Theory, Wiley, New York, 1964.
[29] B. Kumar, M. Beyler, C.P. Kubiak, S. Ott, Chem. Eur. J. 18 (2012) 1295–1298.
[30] Y. Hou, B.L. Abrams, P.C.K. Vesborg, M.E. Bjorketun, K. Herbst, L. Bech, B. Seger, T. Pedersen, O. Hansen, J. Rossmeisl, S. Dahl, J.K. Norskov, I. Chorkendorff, J. Photonics Energy 2 (2012) 026001.
[31] Y. Hou, B.L. Abrams, P.C.K. Vesborg, M.E. Bjorketun, K. Herbst, L. Bech, A.M. Setti, C.D. Damsgaard, T. Pedersen, O. Hansen, J. Rossmeisl, S. Dahl, J.K. Norskov, I. Chorkendorff, Nat. Mater. 10 (2011) 434–438.
[32] Z. Han, L. Shen, W.W. Brennessel, P.L. Holland, R. Eisenberg, J. Am. Chem. Soc. 135 (2013) 14659–14669.
[33] H. Yan, J. Yang, G. Ma, G. Wu, X. Zong, Z. Lei, J. Shi, C. Li, J. Catal. 266 (2009) 165–168.
[34] A. Das, Z. Han, W.W. Brennessel, P.L. Holland, R. Eisenberg, ACS Catal. 5 (2015) 1397–1406.
[35] W.R. McNamara, Z. Han, P.J. Alperin, W.W. Brennessel, P.L. Holland, R. Eisenberg, J. Am. Chem. Soc. 133 (2011) 15368–15371.